Escola de Primavera de Transição e Turbulência
Blumenau 2020

ABCM Associação Brasileira de Engenharia e Ciências Mecânicas

12th Spring School on Transition and Turbulence
September 21st-25th, 2020, Blumenau, SC, Brazil

EPTT-2020-0068
Tollmien-Schlichting waves artificially inserted in boundary layer by harmonic point source

Victor Barcelos Victorino
Christian Salaro Bresci
Matheus Maia Beraldo
Marcello Augusto Faraco de Medeiros
USP, EESC, SAA, zipcode 13566-590
barcelos.victorino@usp.br, christian.bresci@hotmail.com, matheusmberaldo@gmail.com, marcello@sc.usp.br

Abstract. *The present work experimentally investigates the spatial evolution of controlled artificial disturbances inserted by a harmonic point source in Blasius boundary layer over a flat plate. A small hole of 0.80 mm diameter is responsible to introduce inside the boundary layer a blow and suction flow induced by a loudspeaker membrane. The model employed consists of a plexiglass plate with 1800 mm chord, 1000 mm span and 10 mm thickness, vertically assembled inside the test section of the Low Acoustic Noise and Turbulence wind tunnel at EESC-USP. Aluminum leading-edge, flap and tab were attached to model in order to promote a practically constant pressure distribution. Hot-Wire Anemometry was carried out in order to base flow, turbulence level and Tollmien-Schlichting profiles characterization. Good agreement with Blasius was obtained in at least 300 mm span range, on two different streamwise positions. Tollmien-Schlichting eigenfunction profiles were measured for different positions in chordwise direction. Amplification region match the predicted by Linear Stability Theory. Through spectral analysis it was possible to identify the presence of fundamental and first harmonic oscillation, which led to conclusion that the flow conditions contributed to weakly non-linear regime.*

Keywords: *Tollmien-Schlichting Wave, Harmonic Point Source, Transition, Instability*

1. INTRODUCTION

Flow instabilities and the onset of turbulence in boundary layer are characterized by complex nature and chaotic motion. Such dynamics arise from, among several mechanisms, interactions of non-linear effects on oscillations present in flow. Once turbulence regime is reached, time dependent motion promotes mass, momentum and energy transference and as consequence, losses become strongly affected. Therefore, engineering and physical sciences search for better comprehension of the process.

First experimental evidence of flow turbulence was reported by Reynolds (1883). Following, Tollmien (1928) and Schlichting (1933) worked on the development of the Linear Stability Theory (LST), which is based on stability of viscous laminar Blasius boundary layer to small amplitude disturbances. Although, the validity of the LST was achieved only after experimental evidences obtained by Schubauer (1948). The theory is derived from linearized Navier-Stokes equations (LNSE) applied on parallel flows, e.g. two-dimensional boundary layer. Variables are decomposed into time invariant component (base flow) and time dependent small amplitude harmonic oscillation. Non-linear terms are neglected, because it is assumed that the amplitude is small compared to base flow magnitude. After manipulation and the application of normal modes analysis, the equation

$$(\alpha U - \omega)(\phi'' - \alpha^2\phi) - \alpha U''\phi = -\frac{i}{Re_{\delta^*}}(\phi'''' - 2\alpha^2\phi'' + \alpha^4\phi) \tag{1}$$

commonly referred as Orr-Sommerfeld equation, can be treated as an eigenvalue problem.

Originally, the LST treated the problem as temporal and once specified α and Re_{δ^*}, the complex eigenvalue, ω, is solution. This variable represents temporal frequency and its imaginary part $\Im(\omega)$, called amplification factor, determines rather the associated spatial wavenumber, α, at a specific Re_{δ^*} is stable ($\Im(\omega) < 0$) or unstable ($\Im(\omega) > 0$). The eigenfunction, $\phi(y)$, describes the amplitude profile across the wall-normal direction (y) and the instability wave characterized by these parameters is named Tollmien-Schlichting (TS) wave. After several calculations for different combinations of parameters, the instability locus can be mapped and it is usually plotted by means of the neutral stability curve diagram. The minimum Reynolds number based on displacement thickness, Re_{δ^*}, which no amplification occurs it is called critical Reynolds (Re_{crit}) and two branches bound the instability region. Such boundaries correspond to region where $\Im(\omega) = 0$.

It is important to stand out the fact that the perturbations artificially imposed over boundary layer at a fixed streamwise position consist of a spatial problem. Later, Gaster (1962) demonstrated through the Cauchy-Riemann relations that the spatial growth is related to time growth by the group velocity, $c_g = d\omega/d\alpha$.

Schubauer (1948) pointed out that study of TS waves produced by controlled artificial disturbances could be more beneficial than under natural circumstances, e.g. free-stream turbulence. Perturbation source devices of various kind were explored and the vibrating ribbon being the most appropriate accordingly to the authors. Klebanoff *et al.* (1962) also performed experiments through this technique and remarkable contributions were achieved about the three-dimensional nature of TS wave, characterized by spanwise pattern in wave amplitude. The authors stated that the actual breakdown of wave motion to turbulence occurs as consequence of non-linear three-dimensional effects that lead to secondary instabilities by formation of hairpin eddies. Afterward, this regime was named K-type transition.

In addition, other laminar breakdown regime was observed by Kachanov *et al.* (1977), also reported in Kachanov and Levchenko (1984) and Kachanov (1994). In this type of transition, no turbulent spikes of unsteady velocity records were observed, as opposite to Schubauer (1948). The spectral analysis of this transition process lead to a subdivision of four stages. Initially, weakly linear development occurred as well as growth of fundamental frequency harmonics of the perturbation imposed over the flow. Second stage is marked by growth attenuation of these components, whilst appearance of low frequency and sub-harmonic component in spectrum. Subsequently, three-dimensional effects were reported followed by interaction among the low-frequency pulsation, fundamental mode and its harmonics. Lastly, the process presents attenuation of harmonics and laminar breakdown. This kind of transition driven by three-dimensional resonance interactions was called N-type transition.

Gaster (1990) carried out experiments employing a harmonic point source to stimulate TS waves over Blasius boundary layer. The device selected as source was a small loudspeaker buried inside a bore located at opposite surface of flat plate experiment side. Transmission of disturbance to boundary layer flow was due small holes of 0.30 mm diameter in which a blow and suction flow was induced by the loudspeaker. Three types of input signal were investigated: a periodic monochromatic sinusoidal wavetrain, a controlled broadband noise, with low amplitude relative to sinusoidal signal, and a composition of both. Despite no turbulence was reached through regime employed, results exhibited spectrum similar to obtained by Kachanov and Levchenko (1984). The author concluded that large amplitude Tollmien-Schlichting waves are unstable to weak excitations at subharmonic frequency and its multiples. The rate of amplification of the secondary motion were proportional to the square of the fundamental driving signal as expected based on weakly non-linear theory.

The non-linear evolution of a wavetrain was also experimentally investigated by Medeiros (2004). The disturbance amplitude employed was sufficient to promote a weakly non-linear behavior. The results exhibited a three-dimensional mean flow distortion in form of longitudinal streaks. Two distinct stages of the non-linear regime were also reported. The first was characterized by low spanwise wavenumber apparently associated to a pair of counter rotating streamwise vortices. Based on parabolized stability equations (PSE), such flow structures arise from interaction between spanwise and wall-normal modes. The second stage presented more streaks and higher spanwise wavenumber. Streamwise location of this stage onset was not influenced by the input amplitude, although it was associated with second branch of neutral stability diagram.

Present work concerns on experimental study of the development of artificial Tollmien-Schlichting waves over a Blasius boundary layer. The disturbance source device employed was a small loudspeaker, like presented by Gaster (1990) and Medeiros (2004). Such disturbance is characterized by three-dimensional nature and depending on input amplitude, non-linear effects became significant. The eigenfunction profile were measured and spectral analysis was employed. An attempt to identify some aspects related to previously cited references were carried out and LST calculations were applied in order to verify whether the experimental results match the predicted by theory.

2. EXPERIMENTAL SETUP

The current work experiments were performed at Low Acoustic Noise and Turbulence wind tunnel (LANT) present at EESC-USP. Such facility provides a good quality flow for transition study purpose, the free-stream turbulence intensity measured with empty test section is 0.05 %. This accomplishment occurs due to straightening and turbulence attenuation devices, such as honeycomb ducts and screens inside the settling chamber and turning vanes in corners sections. Whilst, acoustic absorber foam present inside the turning vanes and the corners sections of wind tunnel contribute to attenuation of acoustic radiation. The test section possess a squared cross sectional area of 1.00 m^2 and length of 3.00 m. Figure 1 exhibits the blue print of the wind tunnel facility, where the aforementioned devices are highlighted by colored schemes.

The model consists of a plexiglass flat plate (element number 2 in Fig. 2a) with 1800 mm chordwise length, 1000 mm of span and 10 mm of thickness, vertically installed inside test section. An asymmetrical modified super-ellipse leading edge (element number 1 in Fig. 2a) is attached at frontal region of plate , while at trailing edge a flap and tab set (elements number 3 and 4, respectively, in Fig. 2a) are installed, all of them made of aluminum. This last apparatus is used to ensure a good pressure distribution, which is no significant pressure gradient along the experiment envelope region, and to position the stagnation line slightly at work-side. The leading edge geometry was designed to prevent peak suction on work-side surface, and to promote reduced length where the pressure settles after the stagnation (Hanson *et al.*, 2012). The

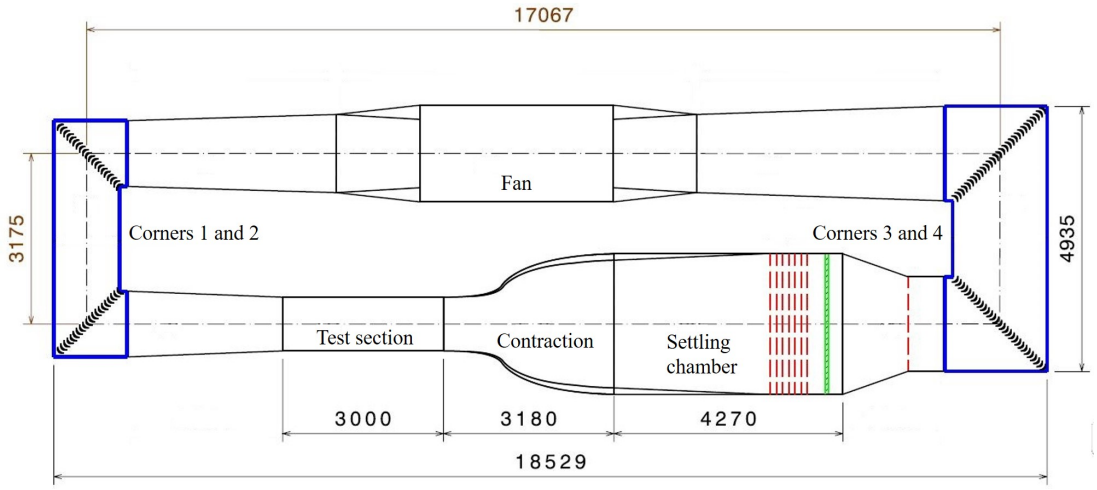

Figure 1. Blue print of LANT wind tunnel. The black C-shaped lines arrays indicates the corning vanes, blue boxes, the region coated by acoustic absorber foam, red dashed lines, the screens and green hatched strip, the honeycomb ducts. Air flows in clockwise direction. Dimensions in millimeters.

pressure distribution was measured through static pressure taps distributed along the model, attached to an inclined U-tube manometer bank. Figure 2a exhibits the isometric view of flat plate model, as well as Fig. 2b displays the leading edge super-elliptical profile.

Located over centerline, 200 mm distant from flat plate leading edge, there is a small through-hole with 0.80 mm diameter concentric with a blind-hole of 8.00 mm diameter with 8.00 mm depth relative to opposite work-side model surface. A loudspeaker was buried inside the cavity of bigger hole and was responsible for excitation of a controlled disturbance into boundary layer flow. The loudspeaker diaphragm was flush to entrance of the small diameter duct, and when driven by a signal input, vibration motion induced a blow and suction flow. This flow was responsible for introduce a harmonic point source of perturbation. The input signal was transmitted by an Agilent 33500B function generator. A sine-like monochromatic wave with 200 Hz frequency and 250 mV amplitude was chosen as input for the flow regime employed.

Hot-Wire Anemometry was the technique selected for velocity measurements. The constant temperature anemometer circuit model DISA 55D01 counts with a DANTEC 55P05 tungsten probe with filament diameter of 5 μm and length of 1 mm. The output signal was branched and transmitted to two acquisition devices. The first consists of 16-bit resolution National Instruments (NI) DAQ USB-6002 module, and it was responsible for recording the DC voltage component. The second instrument, responsible for acquiring AC voltage component signal, was an acquisition board NI 4498, with 24-bit resolution and 114 dB dynamic range, connected to a NI PXI-1042Q chassis. Conditioning and manipulation of signal were performed by MATLAB scripts. The position of probe inside test section was controlled by in-house traverse mechanism. Calibration operation was performed in order to convert voltage into velocity. A script was able to fit the parameter values, through King's Law correlation between the velocity, measured by a static pitot tube placed inside test section, and the output voltage of anemometer. Environment measurements, such as atmospheric pressure, ambient and flow temperature were also employed. The traverse position as well as data acquisition were controlled by computer routines.

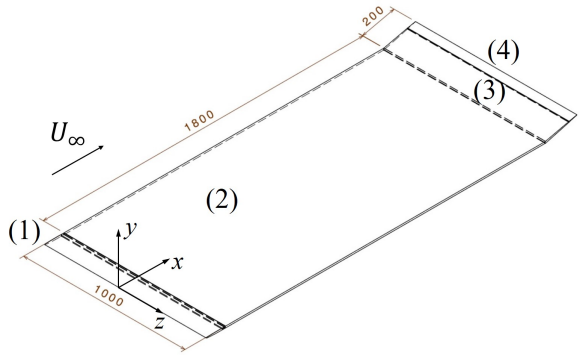

(a) Model.

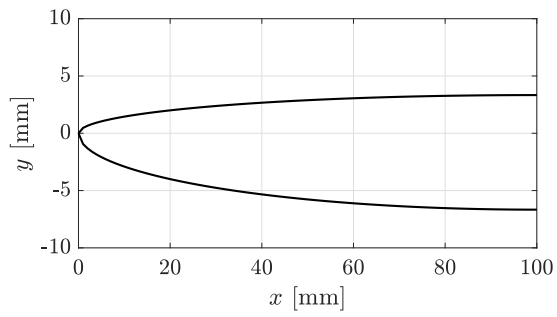

(b) Leading edge.

Figure 2. Isometric view of model and asymmetrical leading edge profile. Dimensions in millimeters.

3. RESULTS

3.1 PRELIMINARY EXPERIMENTS

Preliminary experiments were conducted for base flow verification. Turbulence intensity was measured at position $x = 400$ mm, 150 mm distant from flat plate work-side surface over the centerline. The signal was acquired at rate of 2048 samples/s during 100 seconds, for two different free-stream velocities, $U_\infty = 15$ ms^{-1} and $U_\infty = 20$ ms^{-1}. Two techniques were employed for signal conditioning and turbulence evaluation, respectively. Firstly, the Welch's method (Cryer *et al.* (2010)) was implemented in order to estimate the power spectral density (PSD). Such method reduces frequency resolution to improve signal-to-noise ratio, by reshaping the raw signal into 100 blocks, each one with 1 second of time length, followed by ensemble average of the PSD. The other technique, provided by Lindgren (2002), consists of applying a dynamic filter with cut-off frequency given by $f_c = U_\infty/\lambda_c$. The parameter $\lambda_c = 2$ m was set based on twice the maximum reference length of test section cross-sectional area. Turbulence intensity was calculated by $Tu = u_{rms}/U_\infty$ [%] and root-mean square (RMS) was calculated by square root of PSD sum along the interval given by cut-off and Nyquist frequencies. Figure 3 shows the PSD of free-stream unsteady velocity component. The spectrum behaves as expected. It is possible to note high energy at low-frequency range of approximately $4 - 10$ Hz, typical from closed-circuit wind tunnels and a region with energy decay on range of $0 - 200$ Hz. A smooth peak related to traverse vibration occurs around 140 Hz, however such component did not interfere on results. Sharp peaks associated to power line utility frequency ($f_{pl} = 60$ Hz) and its harmonics ($n \cdot f_{pl}$; n = 1,2,3...), are also noticed. For both velocities, the turbulence intensity measured was $Tu = 0.10\%$, which is suitable for current work.

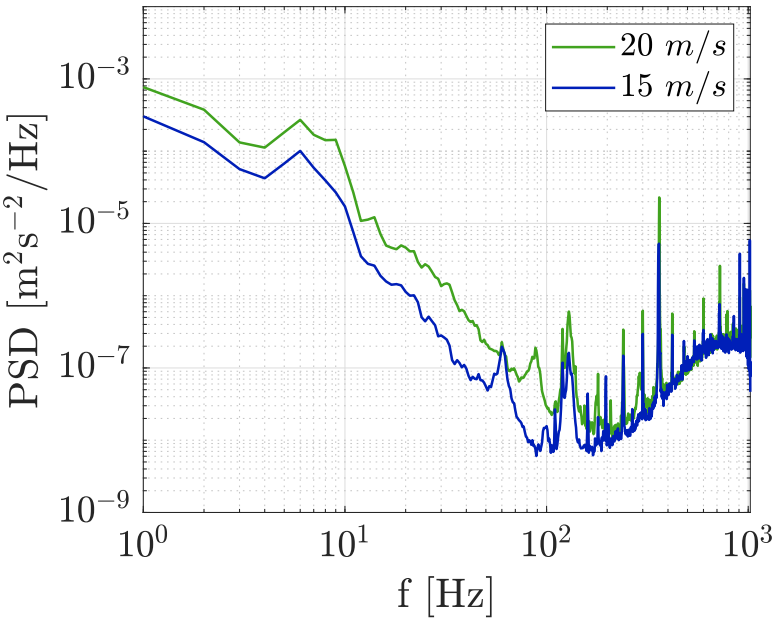

Figure 3. Power spectral density of unsteady free-stream velocity component.

The mean velocity boundary layer profile was measured and compared to Blasius' theory. Two sets of profiles were taken in two distinct streamwise position, $x = 200$ mm and $x = 900$ mm, both with discretization of 30 mm, covering a span (z axis) of 300 mm and 480 mm, respectively. The free-stream velocity was set constant near the velocity employed for TS experiments (≈ 17 ms^{-1}). The discretization in wall-normal direction was set 0.10 mm, at $x = 200$ mm, and 0.20 mm, at $x = 900$ mm. Distance between the measurement point closest to model surface was estimated assuming Blasius profile. Each profile was normalized by the boundary layer edge velocity, calculated by the mean velocity of five most distant points from model surface. The wall-normal direction (y axis) is represented by the similarity parameter $\eta = y\sqrt{U_\infty/\nu x}$. Kinematic viscosity, $\nu = 1.76\ 10^{-5}$ m^{2}s^{-1}, was calculated after dynamic viscosity, given mean flow temperature, and airflow density calculated by ideal gas relation for environmental conditions measured, $\rho = p_{atm}/RT_\infty$. Figure 4 shows the comparison between theoretical Blasius and experimental profiles. It is noted a good agreement with Blasius and high uniformity of boundary layer across the span covered.

3.2 TOLLMIEN-SCHLICHTING WAVES

Six Tollmien-Schlichting amplitude profiles were measured in streamwise (x axis) range of 500 mm $-$ 1000 mm, spaced by 100 mm. The free-stream velocity was set constant at $U_\infty = 17.3$ ms^{-1}. The unsteady velocity records were taken along 31 seconds of time length for each measurement point, with sample rate of 2000 samples/s. Previously cited,

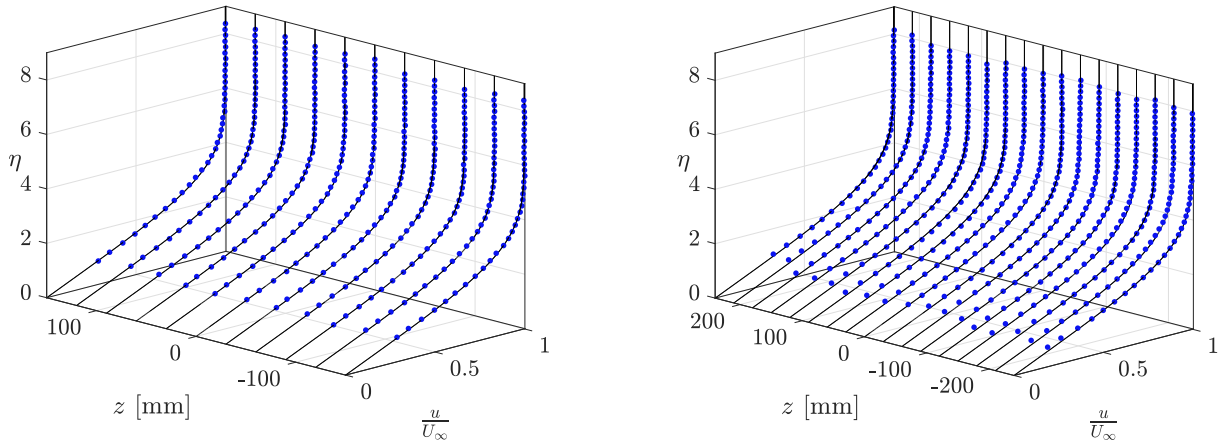

(a) $x = 200$ mm. (b) $x = 900$ mm.

Figure 4. Experimental mean velocity profile (blue dots) along span in comparison with Blasius (black solid lines) for two different chordwise positions.

Welch's method was employed to increase signal-to-noise ratio, by segmenting the raw signal into 35 blocks and taking ensemble average for PSD estimate. The profile amplitude of u' was given by RMS of unsteady record, which was calculated by the square root of PSD summed over narrow interval centered at 200 Hz. Such range covered $\pm 2\Delta f$ wide span, where $\Delta f \approx 1.15$ Hz is the frequency resolution of reshaped signal. The sum interval was chosen based on PSD analisys, it was necessary to include possible power leakage arising from Welch's method, although it should not include undesired energy of other frequency components.

Figure 5 exhibits in (a), normalized profile for each x position, whereas in (b), contours of percentage amplitude relative do free-stream velocity (u'/U_∞ [%]) for the $x\eta$ plane. Analysis of Fig. 5a indicates that the TS peak location gets sharper as it evolves across streamwise direction, which is consistent once the non-normalized amplitude increases downstream as reaches instability. Around the local maximum next to $\eta \approx 4$, one can note a decrease trend of outer peak across the x axis, and after the TS reaches stability at $x > 800$ mm, it seems to appear distortions in this region of amplitude profile. This evidence is showed also in Fig. 5b.

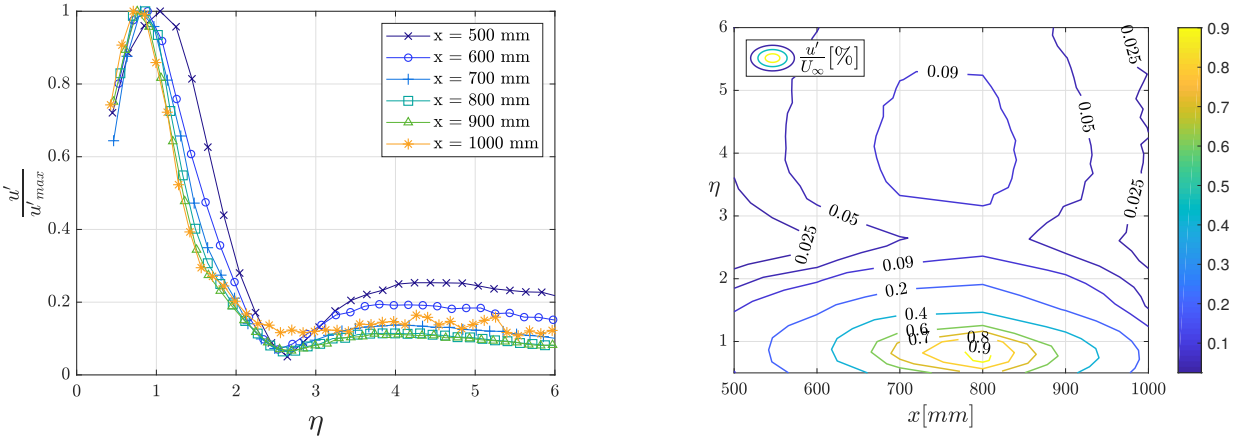

(a) Normalized TS profiles for different chordwise position. (b) Contour of u'/U_∞ [%] amplitude on $x\eta$ plane .

Figure 5. Experimentally measured Tollmien-Schlichting waves.

The TS inner peak spectrum were also investigated and it is showed in Fig. 6 by the dark blue solid lines. Several characteristics concerning stability occurs. Firstly, a bell shaped amplitude values within a frequency band is present in PSD plot of almost all x positions covered. This behavior is expected, once exhibits the disturbances amplification of unstable interval frequencies, which naturally arises inside the boundary layer. The light blue and yellow dash-dot lines displayed in Fig. 6 locate the dimensional frequency of branch I and II of neutral curve stability diagram, respectively. Such values were obtained by in-house codes that evaluate numerically the problem after the Linear Stability Theory (LST). In the range of 500 mm $\leq x \leq$ 800 mm, the branch II frequency practically coincides with the maximum of those bell

shaped bulges, which is expected accordingly to LST. However, once the dominant forced perturbation with frequency 200 Hz is no longer unstable, the behavior of the remaining unstable frequencies apparently changes and the most amplified frequency appears close to center of unstable region delimited by the branches, around 100 Hz.

A sharp peak at 200 Hz it is highlighted by green dashed line in Fig. 6 (a) to (f). As such frequency remains within the range of unstable frequencies, disturbance growth occurs. Secondary instability seem to arose through the 400 Hz harmonic at position $x = 600$ mm, exhibited in Fig. 6 by black dotted line. Amplification of this component also occurs, despite the fact that this frequency is stable.

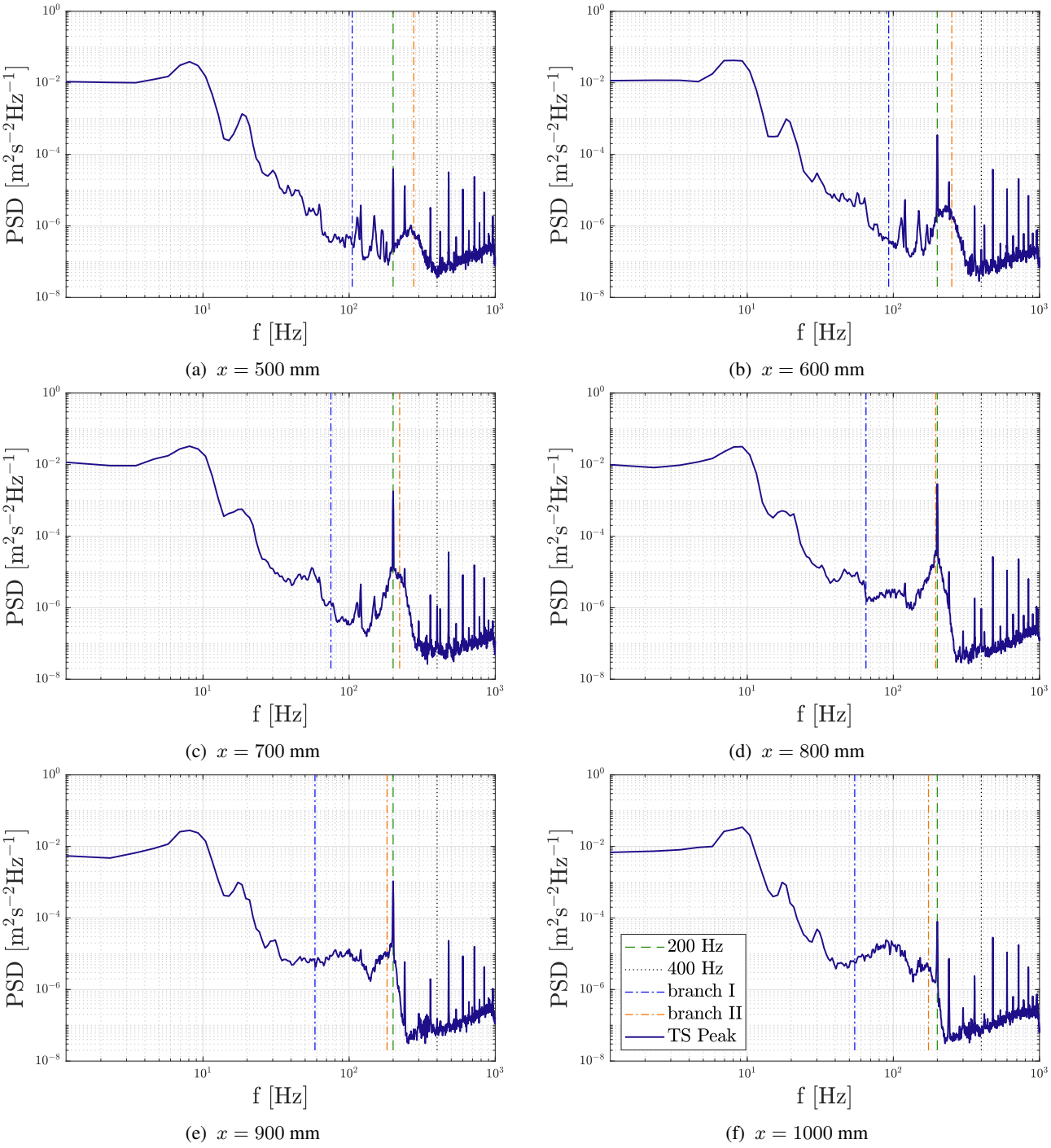

(a) $x = 500$ mm (b) $x = 600$ mm

(c) $x = 700$ mm (d) $x = 800$ mm

(e) $x = 900$ mm (f) $x = 1000$ mm

Figure 6. Power spectral density of TS peak along the streamwise direction x.

4. CONCLUDING REMARKS

Tollmien-Schlichting waves were artificially excited by harmonic point source. The base flow over a flat plate with virtual zero pressure-gradient was characterized, such as the free-stream turbulence intensity. Good agreement with Blasius

was reached and a suitable level of turbulence was obtained. It was possible to measure the eigenfunction amplitude profile. Amplitude growth occurred inside unstable region predicted by LST, as well as damping at positions downstream the branch II of neutral curve. By analysis of PSD corresponding to the TS peak location, it was possible to identify some aspects provided by Gaster (1990) and Kachanov *et al.* (1977). Among which, was possible to notice the presence of first harmonic of fundamental disturbance (400 Hz). This component should not be amplified, once it is located in stable locus of stability diagram, however growth was observed. Apparently, this component arises from non-linear interactions and its amplitude is related to the amplitude of fundamental disturbance (200 Hz). Low frequencies around the sub-harmonic (100 Hz) also presented amplification at downstream positions. As pointed by Gaster (1990), this fact could be associated with the instability of relative large amplitude TS waves to small perturbations within frequencies close to sub-harmonic component.

5. ACKNOWLEDGEMENTS

V.B.V. was funded from CNPq/Brazil, grant 134335/2018-0. C.S.B. was funded by CAPES/Brazil, under the CAPES/PROAP Social Demand program. M.M.B. was funded by CAPES/Brazil, grant 88882.379172/2019-1. M.A.F.M. thanks the National Council for Scientific and Technological Development (CNPq/Brazil) for grants 307956/2019-9 and the US Air Force Office of Scientific Research (AFOSR) for grant FA9550-18-1-0112, managed by Dr. Geoff Andersen from SOARD. The LANT wind-tunnel financial support was provided by FINEP/Brazil, grant 01.09.0334.04. The authors also thanks FAPESP/Brazil for grant 2019/15366-7.

6. REFERENCES

Cryer, J.D., Bendat, J.S. and Piersol, A.G., 2010. *Random Data - Analysis and Measurement Procedures*, Vol. 82. JOHN WILEY & SONS, INC., 4th edition. ISBN 9780470248775. doi:10.2307/2289430.

Gaster, M., 1962. "A note on the relation between temporally-increasing and spatially-increasing disturbances in hydrodynamic stability". *Journal of Fluid Mechanics*, Vol. 14, No. 2, pp. 222–224. ISSN 14697645. doi:10.1017/S0022112062001184.

Gaster, M., 1990. "The nonlinear phase of wave growth leading to chaos and breakdown to turbulence in a boundary layer as an example of an open system". *Proceedings of the Royal Society of London. Series A: Mathematical and Physical Sciences*, Vol. 430, No. 1878, pp. 3–24. ISSN 0962-8444. doi:10.1098/rspa.1990.0078.

Hanson, R.E., Buckley, H.P. and Lavoie, P., 2012. "Aerodynamic optimization of the flat-plate leading edge for experimental studies of laminar and transitional boundary layers". *Experiments in fluids, Springer*, Vol. 53, No. 4, pp. 863–871. doi:10.1007/s00348-012-1324-2.

Kachanov, Y.S., Kozlov, V.V. and Levchenko, V.Y., 1977. "Nonlinear development of a wave in a boundary layer". *Fluid Dynamics*, Vol. 12, No. 3, pp. 383–390. ISSN 15738507. doi:10.1007/BF01050568.

Kachanov, Y.S. and Levchenko, V.Y., 1984. "The resonant interaction of disturbances at laminar-turbulent transition in a boundary layer". *Journal of Fluid Mechanics*, Vol. 138, No. 1984, pp. 209–247. ISSN 14697645. doi:10.1017/S0022112084000100.

Kachanov, Y.S., 1994. "Physical mechanisms of laminar-boundary-layer transition". *Annual Review of Fluid Mechanics*, Vol. 26, pp. 411–482.

Klebanoff, P.S., Tidstrom, K.D. and Sargent, L.M., 1962. "The three-dimensional nature of boundary-layer instability". *Journal of Fluid Mechanics*, Vol. 12, No. 1, pp. 1–34. ISSN 14697645. doi:10.1017/S0022112062000014.

Lindgren, Björn Johansson, A.V., 2002. "Evaluation of the flow quality in the mtl wind-tunnel". Technical report, Royal Institute of Technology Department of Mechanics, SE-100 44 Stockholm, Swede. URL `https://www.mech.kth.se/~oso/papers/MTL_techrep.pdf`.

Medeiros, M.A.F., 2004. "The nonlinear evolution of a wavetrain emanating from a point source in a boundary layer". *Journal of Fluid Mechanics*, Vol. 508, pp. 287–317. doi:10.1017/S0022112004009188.

Reynolds, O., 1883. "An Experimental Investigation of the Circumstances Which Determine Whether the Motion of Water Shall Be Direct or Sinuous, and of the Law of Resistance in Parallel Channels". In *Philosophical Transactions of the Royal Society of London*. Vol. 35, pp. 84–99. ISSN 0261-0523. doi:10.1098/rstl.1883.0029.

Schlichting, H., 1933. "Laminare Strahlausbreitung". *ZAMM - Journal of Applied Mathematics and Mechanics / Zeitschrift für Angewandte Mathematik und Mechanik*, Vol. 13, No. 4, pp. 260–263. ISSN 15214001. doi:10.1002/zamm.19330130403.

Schubauer, G.B. Skramstad, H., 1948. "Laminar-Boundary-Layer Oscillations and Transition on a Flat Plate". Technical Report 909, National Advisory Committee for Aeronautics, Washington, US. URL `https://ntrs.nasa.gov/search.jsp?R=19930091976`.

Tollmien, W., 1928. "Über die Entstehung der Turbulenz. 1. Mitteilung". *Nachrichten von der Gesellschaft der Wissenschaften zu Göttingen, Mathematisch-Physikalische Klasse*, Vol. 1929, pp. 21–44. URL `http://eudml.org/doc/59276`.

7. RESPONSIBILITY NOTICE

The authors are the only responsible for the printed material included in this paper.